

This discussion paper is/has been under review for the journal Biogeosciences (BG).
Please refer to the corresponding final paper in BG if available.

Fate of peat-derived carbon and associated CO₂ and CO emissions from two Southeast Asian estuaries

D. Müller^{1,2}, T. Warneke¹, T. Rixen^{2,3}, M. Müller⁴, A. Mujahid⁵, H. W. Bange⁶, and J. Notholt¹

¹Institute of Environmental Physics, University of Bremen, Otto-Hahn-Allee 1, 28359 Bremen, Germany

²Leibniz Center for Tropical Marine Ecology, Fahrenheitstr. 6, 28359 Bremen, Germany

³Institute of Geology, University of Hamburg, Bundesstr. 55, 20146 Hamburg, Germany

⁴Swinburne University of Technology, Faculty of Engineering, Computing and Science, Jalan Simpang Tiga, 93350 Kuching, Sarawak, Malaysia

⁵Department of Aquatic Science, Faculty of Resource Science and Technology, University Malaysia Sarawak, 94300 Kota Samarahan, Sarawak, Malaysia

⁶GEOMAR Helmholtz Centre for Ocean Research Kiel, Düsternbrooker Weg 20, 24105 Kiel, Germany

BGD

12, 8299–8340, 2015

CO₂ and CO emissions from Southeast Asian estuaries

D. Müller et al.

[Title Page](#)

[Abstract](#)

[Introduction](#)

[Conclusions](#)

[References](#)

[Tables](#)

[Figures](#)

◀

▶

◀

▶

[Back](#)

[Close](#)

[Full Screen / Esc](#)

[Printer-friendly Version](#)

[Interactive Discussion](#)



Received: 4 May 2015 – Accepted: 13 May 2015 – Published: 5 June 2015

Correspondence to: D. Müller (dmueller@iup.physik.uni-bremen.de)

Published by Copernicus Publications on behalf of the European Geosciences Union.

BGD

12, 8299–8340, 2015

Discussion Paper | Discussion Paper

CO₂ and CO emissions from Southeast Asian estuaries

D. Müller et al.

[Title Page](#)

[Abstract](#)

[Introduction](#)

[Conclusions](#)

[References](#)

[Tables](#)

[Figures](#)

◀

▶

[◀](#)

[▶](#)

[Back](#)

[Close](#)

[Full Screen / Esc](#)

[Printer-friendly Version](#)

[Interactive Discussion](#)

Abstract

Coastal peatlands in Southeast Asia release large amounts of organic carbon to rivers, which transport it further to the adjacent estuaries. However, little is known about the fate of this terrestrial material in the coastal ocean. Although Southeast Asia is, by area, considered a hotspot of estuarine CO_2 emissions, studies in this region are very scarce. We measured dissolved and particulate organic carbon, carbon dioxide (CO_2) partial pressure and carbon monoxide (CO) concentrations in two tropical estuaries in Sarawak, Malaysia, whose coastal area is covered by peatlands. We surveyed the estuaries of the rivers Lumar and Saribas during the wet and dry season, respectively. The spatial distribution and the carbon-to-nitrogen ratios of dissolved organic matter (DOM) suggest that peat-draining rivers convey terrestrial organic carbon to the estuaries. We found evidence that a large fraction of this carbon is respired. The median $p\text{CO}_2$ in the estuaries ranged between 618 and 5064 μatm with little seasonal variation. CO_2 fluxes were determined with a floating chamber and estimated to amount to 14–272 $\text{mol m}^{-2} \text{yr}^{-1}$, which is high compared to other studies from tropical and subtropical sites. In contrast, CO concentrations and fluxes were relatively moderate (0.3–1.4 nmol L^{-1} and 0.8–1.9 $\text{mmol m}^{-2} \text{yr}^{-1}$) if compared to published data for oceanic or upwelling systems. We attributed this to the large amounts of suspended matter (4–5004 mg L^{-1}), limiting the light penetration depth. However, the diurnal variation of CO suggests that it is photochemically produced, implying that photodegradation might play a role for the removal of DOM from the estuary as well. We concluded that unlike smaller peat-draining tributaries, which tend to transport most carbon downstream, estuaries in this region function as an efficient filter for organic carbon and release large amounts of CO_2 to the atmosphere. The Lumar and Saribas mid-estuaries release $0.4 \pm 0.2 \text{ Tg C yr}^{-1}$, which corresponds to approximately 80 % of the emissions from the aquatic systems in these two catchments.

CO₂ and CO emissions from Southeast Asian estuaries

D. Müller et al.

[Title Page](#)

[Abstract](#)

[Introduction](#)

[Conclusions](#)

[References](#)

[Tables](#)

[Figures](#)

◀

▶

◀

▶

[Back](#)

[Close](#)

[Full Screen / Esc](#)

[Printer-friendly Version](#)

[Interactive Discussion](#)



1 Introduction

Southeast Asian peatlands store 68.5 Gt carbon (Page et al., 2011) and represent a globally important carbon pool. Parts of this organic carbon are released to the aquatic system and exported to the coastal ocean. It has been estimated that due to the presence of peatlands, Indonesia alone accounts for 10 % of the dissolved organic carbon (DOC) exported to the ocean globally (Baum et al., 2007). Peat-draining rivers usually exhibit extraordinarily high DOC concentrations (Alkhatib et al., 2007; Moore et al., 2011, 2013; Müller et al., 2015). Although a small fraction of this DOC is respired in the river, the larger part is transported downstream (Müller et al., 2015), ultimately reaching the estuary and the coastal ocean. So far, the fate of this carbon fraction remains unclear, and data particularly in this region is scarce.

Globally, the view prevails that terrestrial organic carbon is respired in estuaries. Therefore, they are net heterotrophic (Duarte and Prairie, 2005) and act as a source of carbon dioxide (CO_2) to the atmosphere, releasing 150 Tg C annually (Laruelle et al., 2013). On the other hand, Cai (2011) suggested that terrestrial organic carbon might in fact bypass the estuarine zone, and that it is actually organic carbon from intertidal flats that sustains net heterotrophy in estuaries.

The question whether or not the terrestrial organic carbon is retained in estuaries is of particular interest in peat-dominated regions with high riverine carbon loads like Southeast Asia. On the one hand, peat-derived organic matter consists mainly of lignin and its derivates (Andriesse, 1988) and is thus relatively recalcitrant to degradation. In addition, short water residence times might constrain organic matter decomposition (Müller et al., 2015). On the other hand, high organic carbon loads together with high temperatures would suggest high microbial activity both in the water column and in the sediment, leading to high decomposition rates.

Additionally, photodegradation was proposed as an important removal mechanism for terrestrial organic matter in the ocean (Miller and Zepp, 1995). Chromophoric dissolved organic matter (CDOM) absorbs light, mainly in the UV region. The absorbed

BGD

12, 8299–8340, 2015

CO₂ and CO emissions from Southeast Asian estuaries

D. Müller et al.

[Title Page](#)

[Abstract](#)

[Introduction](#)

[Conclusions](#)

[References](#)

[Tables](#)

[Figures](#)

◀

▶

◀

▶

[Back](#)

[Close](#)

[Full Screen / Esc](#)

[Printer-friendly Version](#)

[Interactive Discussion](#)



photons initiate abiotic photochemical reactions, during which DOC is oxidized to carbon monoxide (CO) and CO₂ (Stubbins, 2001), with the CO₂ production being 14 to 20 times larger than CO production (Vähäntalo, 2010). Photochemistry might be of particular importance in estuaries (Ohta et al., 2000), where CDOM concentrations and 5 CO production rates are high, making estuaries a significant source of CO to the atmosphere (Valentine and Zepp, 1993). What adds to it, is that dissolved organic matter (DOM) in estuaries is largely of terrestrial origin, and terrestrial CDOM was found to be more efficient in producing CO than marine CDOM (Zhang et al., 2006). Ultimately, 10 recalcitrant peat-derived organic matter might be subject to photobleaching (Vähäntalo, 2010) and would then be more readily available for bacterial respiration, supporting net heterotrophy.

In order to investigate if and how peat-derived organic carbon is processed in tropical estuaries, we studied organic carbon, dissolved CO₂ and CO in two Malaysian estuaries, both of which receive terrestrial carbon from rivers draining a peat-dominated 15 catchment.

2 Materials and methods

2.1 Study area

Sarawak is Malaysia's largest state and located in the northwest of the island of Borneo, which is divided between Indonesia, Brunei and Malaysia. It is separated from Peninsular 20 Malaysia by the South China Sea. Sarawak has a tropical climate. The mean annual air temperature in Sarawak's capital Kuching (1.56° N, 110.35° E) is 26.1 °C (average 1961–1990, DWD, 2007). Rainfall is high throughout the year, but pronounced during the northeast monsoon, which occurs between November and February.

Our study focused on two macrotidal estuaries in western Sarawak. The coastal 25 area of western Sarawak is covered by peatlands. The largest peat dome is found on the Maludam peninsula. It is rainwater-fed and covered by dense peat swamp forest,

CO₂ and CO emissions from Southeast Asian estuaries

D. Müller et al.

[Title Page](#)

[Abstract](#)

[Introduction](#)

[Conclusions](#)

[References](#)

[Tables](#)

[Figures](#)

◀

▶

◀

▶

[Back](#)

[Close](#)

[Full Screen / Esc](#)

[Printer-friendly Version](#)

[Interactive Discussion](#)



which has been protected ever since Maludam was gazetted as national park in 2000. The peninsula is enclosed by the rivers Lumar and Saribas (Fig. 1). Six channels from the Maludam peat swamp forest drain into the Lumar river and six into the Saribas, respectively (Kselik and Liong, 2004). With reference to their catchment areas, the 5 peat coverage in the Lumar and Saribas basins is 30.5 and 35.5 %, respectively (FAO, 2009). The catchment sizes are 6558 km^2 (Lumar) and 1943 km^2 (Saribas) (Lehner et al., 2006).

Sampling was performed during two ship cruises in 2013 and 2014. The 2013 cruise took place in June (18–23 June) during the dry season. The 2014 cruise was performed 10 in March (10–19 March), right after the end of the monsoon season. We sampled 20 stations in 2013 and 26 stations in 2014 (Fig. 1). Here, we report the data separately for the outer (salinity > 25), mid-(salinities 2–25) and upper estuaries (salinity < 2). In 15 2014, we went further upstream than in 2013. Therefore, when it comes to the mid-estuaries, we report medians for the “2013 spatial extent”, i.e. refer to the spatial coverage of 2013.

2.2 Discharge and flow velocity

We estimated river discharge (Q) from the difference between precipitation (P) and evapotranspiration (ET). Precipitation was taken from NOAA NCEP Reanalysis data set for the nearest upstream grid (0.95°N , 110.625°E , www.esrl.noaa.gov/psd/data/reanalysis/reanalysis.shtml). Evapotranspiration was taken from the literature (Kumagai et al., 2005). Ultimately, we derived $Q = (P - \text{ET}) \cdot A$, where A is the catchment area (m^2). The rivers' flow velocity was estimated from the drift during the stations, when the 20 boat drifted freely. To this end, we used the GPS information of a CTD at the beginning and the end of the cast, and the duration of the cast to calculate the flow velocity (2014 25 data only).

CO₂ and CO emissions from Southeast Asian estuaries

D. Müller et al.

[Title Page](#)

[Abstract](#)

[Introduction](#)

[Conclusions](#)

[References](#)

[Tables](#)

[Figures](#)

◀

▶

◀

▶

[Back](#)

[Close](#)

[Full Screen / Esc](#)

[Printer-friendly Version](#)

[Interactive Discussion](#)



2.3 Water chemistry

Salinity and temperature profiles were measured at each station with a CastAway CTD. Additionally, water pH, dissolved oxygen (DO) and conductivity were measured in the surface water with a WTW Multi3420, using an FDO 925 oxygen sensor, a SenTix 940 5 pH sensor and a TetraCon 925 conductivity sensor. Apparent oxygen utilization (AOU) was calculated as the difference between the saturation oxygen concentration and the measured oxygen concentration.

$$\text{AOU} = \text{O}_2^{\text{sat}} - \text{O}_2^{\text{meas}} \quad (1)$$

Oxygen solubility for a given temperature and salinity was calculated with constants 10 from Weiss (1970).

Samples for determination of dissolved inorganic nitrogen (DIN) concentrations were taken at every station from approximately 1 m below the water surface. The water was filtered through a Whatman glass microfibre filter (pore size 0.7 µm), preserved with a mercuric chloride (HgCl_2) solution and stored cooled and upright until analysis. Concentrations of nitrate (NO_3^-), nitrite (NO_2^-) and ammonia (NH_4^+) were determined spectrophotometrically (Grasshoff et al., 1999) with an Alliance Continuous Flow Analyzer. 15

2.4 Organic carbon and carbon isotope analysis

Dissolved organic carbon (DOC) samples were filtered (pore size 0.45 µm) and acidified with 21 % phosphoric acid until the pH had dropped below 2. DOC concentrations 20 were determined through high temperature combustion and subsequent measurement of the evolving CO_2 with a non-dispersive infrared detector. In 2014, those samples were also analyzed for total dissolved nitrogen (TDN) using a Shimadzu TOC-VCSH with TNM-1 analyzer. Dissolved organic nitrogen (DON) was then calculated by subtracting DIN from TDN.

25 Particulate material was sampled by filtering water through pre-weighed and pre-combusted Whatman glass fiber filters. The net sample weight was determined. 1 N

[Title Page](#)

[Abstract](#)

[Introduction](#)

[Conclusions](#)

[References](#)

[Tables](#)

[Figures](#)

[◀](#)

[▶](#)

[◀](#)

[▶](#)

[Back](#)

[Close](#)

[Full Screen / Esc](#)

[Printer-friendly Version](#)

[Interactive Discussion](#)



hydrochloric acid was added in order to remove inorganic carbon and samples were dried at 40 °C. Organic carbon and nitrogen contents were determined by flash combustion with a Euro EA3000 Elemental Analyzer. The abundance of the stable isotope ^{13}C was determined with a Finnigan Delta plus mass spectrometer.

5 Samples for determination of $\delta^{13}\text{C}$ in dissolved inorganic carbon (DIC) were preserved with HgCl_2 , sealed against ambient air and stored cool, upright and in the dark until analysis. Vials were prepared with 50 μL of 98 % H_3PO_4 and a He headspace. Depending on the salinity, 1–4 mL sample volume was injected through the septum using a syringe. The prepared sample was allowed to equilibrate for 18 h and $\delta^{13}\text{C}$ was 10 determined with a Thermo Scientific mass spectrometer (MAT 253).

2.5 CO_2 and CO measurements

In order to determine partial pressures of dissolved CO_2 and CO in the water, we used a Weiss equilibrator (Johnson, 1999). Water from approximately 1 m below the surface was pumped through the equilibrator at a rate of approximately 20 L min^{-1} . Dry air 15 mole fractions of CO_2 and CO in the equilibrator's headspace were determined with an in-situ Fourier Transform InfraRed (FTIR) trace gas analyzer. The instrument was manufactured at the University of Wollongong, Australia, and is described in detail by Griffith et al. (2012). FTIR spectra were averaged over five minutes, and dry air mole fractions were retrieved using the software MALT5 (Griffith, 1996). The gas dry air 20 mole fractions were corrected for pressure, water and temperature cross-sensitivities with empirically determined factors (Hammer et al., 2013). Calibration was performed twice during each ship cruise with a suite of secondary standards ranging from 380 to 10 000 ppm CO_2 and 51 to 6948 ppb CO. The relevant concentration range was re-evaluated after the cruises.

25 The equilibrator headspace air circulated between the FTIR and the equilibrator at a rate of 1 L min^{-1} in a closed loop, allowing for continuous monitoring of the CO_2 and CO mixing ratios in the headspace. The equilibrator and the sampling lines were covered with aluminum foil to avoid CO photoproduction in the sampled air. Water

BGD

12, 8299–8340, 2015

[Title Page](#)

[Abstract](#)

[Introduction](#)

[Conclusions](#)

[References](#)

[Tables](#)

[Figures](#)

◀

▶

◀

▶

[Back](#)

[Close](#)

[Full Screen / Esc](#)

[Printer-friendly Version](#)

[Interactive Discussion](#)



temperature was measured both in the equilibrator and in the water using a Pico PT-104 temperature data recorder. Ambient air temperature and pressure were recorded over the entire cruise with a Vaisala SP-1016 temperature data recorder and a PTB110 barometer, respectively. Gas partial pressures for dry air ($p\text{Gas}_{\text{dryair}}$) were calculated from the FTIR measurements and our records of ambient pressure. We corrected for the removal of water (Dickson et al., 2007) using

$$p\text{Gas} = p\text{Gas}_{\text{dryair}}(1 - \text{VP}(\text{H}_2\text{O})), \quad (2)$$

where $p\text{Gas}$ is the corrected gas partial pressure and $\text{VP}(\text{H}_2\text{O})$ is the water vapor pressure, which was calculated with the equation given in Weiss and Price (1980).

Equilibrator measurements have been widely used for trace gas measurements in estuarine surface water (Chen et al. (2013) and references therein). For CO_2 , the response time is usually short (< 10 min) and the error associated with a remaining disequilibrium between water and headspace air is 0.2 % for a Weiss equilibrator (Johnson, 1999). CO , in contrast, takes much longer to reach full equilibrium, and an error of up to 25 % must be taken into account for measurements with a Weiss equilibrator (Johnson, 1999).

In the freshwater region, we were unable to carry out FTIR measurements, because the sampling spots could not be reached by ship. Instead, we performed headspace equilibration measurements of discrete samples with an Li-820 CO_2 analyzer, which was calibrated with the same secondary standards as the FTIR. We filled a 10 L canister with 9.5 L of sample water (2014: 0.6 L flask filled with 0.35 L of sample water) and left ambient air in the headspace. We connected the Li-820 analyzer inlet to the headspace and the outlet to the bottom of the canister, so that air could bubble through the sample water, accelerating the equilibration process. The $p\text{CO}_2$ obtained from headspace equilibration measurements was corrected for water vapor pressure as well.

CO₂ and CO emissions from Southeast Asian estuaries

D. Müller et al.

[Title Page](#)

[Abstract](#)

[Introduction](#)

[Conclusions](#)

[References](#)

[Tables](#)

[Figures](#)

◀

▶

◀

▶

[Back](#)

[Close](#)

[Full Screen / Esc](#)

[Printer-friendly Version](#)

[Interactive Discussion](#)



Following common practice, we will report CO₂ levels in terms of CO₂ partial pressure ($p\text{CO}_2$), but convert CO partial pressure to molar concentrations using solubilities according to Wiesenburg and Guinasso (1979).

2.6 Flux estimation

5 In 2014, we performed direct flux measurements with a floating chamber (FC). The FC was an upside-down flower pot with a volume of 8.7 L and a surface area of 0.05 m² which it enclosed with the water. Its walls extended 1 cm into the water. The chamber headspace was connected to the Li-820 CO₂ analyzer, and CO₂ concentrations in the chamber were recorded over time. The concentration change was fitted linearly and
10 the water-to-air CO₂ flux F (in $\mu\text{mol m}^{-2} \text{s}^{-1}$) was calculated according to

$$F = \frac{dc}{dt} \frac{pV}{RTA}, \quad (3)$$

where $\frac{dc}{dt}$ is the slope of the fitted curve ($\mu\text{mol mol}^{-1} \text{s}^{-1}$), p is the pressure (Pa), V is the chamber volume (m³), R is the universal gas constant, T the temperature (K) and A the surface area (m²). The gas exchange velocity was calculated with

$$15 k_{\text{CO}_2} = \frac{F}{K_0 (p\text{CO}_2^{\text{water}} - p\text{CO}_2^{\text{air}})}, \quad (4)$$

where k_{CO_2} is the gas exchange velocity (m s⁻¹) of CO₂ and $p\text{CO}_2^{\text{air}}$ is the atmospheric CO₂ partial pressure, which was measured with the Li-820 CO₂ analyzer during the cruises. For comparisons, k_{CO_2} was normalized to a Schmidt number of 600 (Schmidt number Sc relates the diffusivity of the gas to the viscosity of the water):

$$20 \frac{k_{600}}{k_{\text{CO}_2}} = \left(\frac{600}{\text{Sc}_{\text{CO}_2}} \right)^{-n} \quad (5)$$

BGD

12, 8299–8340, 2015

[Title Page](#)

[Abstract](#)

[Introduction](#)

[Conclusions](#)

[References](#)

[Tables](#)

[Figures](#)

[◀](#)

[▶](#)

[◀](#)

[▶](#)

[Back](#)

[Close](#)

[Full Screen / Esc](#)

[Printer-friendly Version](#)

[Interactive Discussion](#)



with $n = 0.5$ for rough surfaces (Jähne et al., 1987). The relationship with the Schmidt number was also exploited for calculating CO fluxes. Schmidt numbers were calculated from water temperature for both saline and freshwater (CO₂: Wanninkhof (1992), CO: Raymond et al. (2012) for freshwater, Zafiriou et al. (2008) for saltwater), and evaluated for the in-situ salinity assuming a linear dependency (Borges et al., 2004). Atmospheric CO mole fractions were obtained from the NOAA ESRL Carbon Cycle Cooperative Global Air Sampling for the nearest station (Novelli and Masarie, 2014), which was Bukit Kotobatang, Indonesia (0.202° S, 100.3° E).

Since many flux estimates in the literature were obtained using exchange velocities derived from empirical equations, we calculated k also using the wind speed parameterization from Wanninkhof (1992) for comparison. Wind speed data were taken from the NOAA NCEP Reanalysis data set for the closest coastal grid (2.85° N, 110.625° W). Here, we chose the most downstream grid because the upstream grid, which we picked for precipitation, is over land, where wind speeds might be much lower than in the estuary. We considered daily wind speeds for the time period of both our 2013 and 2014 cruise.

3 Results

3.1 Discharge

Annual average precipitation from 1980–2014 amounted to 3903 mm yr⁻¹ in the chosen grid, corresponding to an average precipitation of 325 mm month⁻¹. The precipitation during June 2013 was below average (246 mm) and above average (364 mm) in March 2014. Both values do not deviate much from the historical averages during 1980–2014 (March: 367 mm, June: 234 mm, see Fig. 2). In the following, we will refer to our measurements in June 2013 as representative of the dry season, and those in March 2014 as representative of the wet season.

With an average evapotranspiration of 4.2 mm d^{-1} (Kumagai et al., 2005), we estimated the average annual discharge for the Lumar river to be 490 and $160 \text{ m}^3 \text{s}^{-1}$ for the Saribas river. The flow velocities were estimated to be $2.5 \pm 1.4 \text{ m s}^{-1}$ (average \pm largest deviation from average) for the Lumar river, $0.7 \pm 0.7 \text{ m s}^{-1}$ for the Saribas and $0.8 \pm 1.0 \text{ m s}^{-1}$ for the Saribas tributary. Note that the measurements were taken during different stages of the tidal cycle, which explains the large variability.

3.2 Water chemistry

Our data covered a salinity range of 0–30.6 in 2013 and 0–31.0 in 2014. pH ranged between 6.7 and 8.0 in the dry season (2013) and between 6.8 and 7.6 in the wet season (2014) and was positively correlated with salinity ($r = 0.8$, data from both years). Notably, at salinity zero, pH was higher than suggested by this correlation, and ranged between 6.7 to 7.3 (both seasons).

DIN concentrations were generally rather low. During the dry season, DIN ranged between 1.7 and $87.1 \mu\text{mol L}^{-1}$, whereas most concentrations were between 15 and $30 \mu\text{mol L}^{-1}$. In the wet season, DIN concentrations ranged between 3.4 and $21.7 \mu\text{mol L}^{-1}$. The medians for the individual estuaries show that overall, DIN concentrations were slightly higher in the dry season (Table 1).

Dissolved oxygen was mostly slightly undersaturated. Oxygen saturation was lower in the dry season than in the wet season (Table 1), with oxygen saturation ranging between 63.6 to 94.6 % (2013) and 79.0–100.4 % (2014). These values correspond to an AOU between 14 and $93 \mu\text{mol L}^{-1}$ (2013) and -1 and $52 \mu\text{mol L}^{-1}$ (2014), respectively. Negative AOU suggests net oxygen production and was only observed once in the outer estuary.

3.3 Organic carbon

DOC ranged from 80 to $784 \mu\text{mol L}^{-1}$ in the dry season and from 172 to $1180 \mu\text{mol L}^{-1}$ in the wet season and was negatively correlated with salinity (Fig. 3), indicating that

[Title Page](#)

[Abstract](#)

[Introduction](#)

[Conclusions](#)

[References](#)

[Tables](#)

[Figures](#)

◀

▶

◀

▶

[Back](#)

[Close](#)

[Full Screen / Esc](#)

[Printer-friendly Version](#)

[Interactive Discussion](#)



freshwater supplies DOC to the estuary, while seawater has a dilution effect. However, the end-member determined from the salinity-DOC correlation was not confirmed by the samples taken in the upper estuaries: the calculated end-member for Lumar was $673 \pm 274 \mu\text{mol L}^{-1}$ (intercept of the regression curve \pm standard error of the estimate), the measured freshwater DOC median was $89 \mu\text{mol L}^{-1}$ (2013) and $208 \mu\text{mol L}^{-1}$ (2014). For Saribas, the calculated endmember was $425 \pm 54 \mu\text{mol L}^{-1}$, and the measured value was $312 \mu\text{mol L}^{-1}$ (2013, Table 1). This discrepancy is owed to the fact that the peatlands, which are likely the main source of allochthonous organic carbon, are located in the coastal area, downstream of our freshwater stations (Fig. 1).
 5 In a different study, we found DOC concentrations in a peat-draining river on the Maludam peninsula between 3612 and $3768 \mu\text{mol L}^{-1}$ (Müller et al., 2015). With the average ($3690 \mu\text{mol L}^{-1}$) as a second zero-salinity end-member, we estimated how much carbon derives from peat-draining tributaries from the Maludam peninsula using a simple three-point mixing model (Fig. 3). The Maludam contribution f (in %) was calculated as
 10

$$f = \frac{\text{EM}_{\text{calc}} - \text{EM}_{\text{meas}}}{\text{EM}_{\text{Maludam}} - \text{EM}_{\text{meas}}} \cdot 100, \quad (6)$$

15 with EM_{calc} the calculated end-member, EM_{meas} the measured end-member and $\text{EM}_{\text{Maludam}}$ the peat-draining rivers' end-member. Accordingly, 15 % of the DOC in the Lumar river is derived from peat-draining tributaries, and 3 % of DOC in the Saribas river. The total DOC export to the ocean from Lumar and Saribas was estimated from
 20 the calculated zero-salinity end-members (673 and $425 \mu\text{mol L}^{-1}$, respectively), assuming that they provide an average of non-peat and peat freshwater inputs, and annual average discharge. Accordingly, Lumar and Saribas together convey $0.15 \pm 0.05 \text{ Tg yr}^{-1}$ DOC to the South China Sea (Table 4).

25 Both the Lumar and the Saribas estuary were very turbid. Suspended particulate matter (SPM) ranged from 3.7 to 5003.6 mg L^{-1} in 2013 and from 13.8 to 3566.7 mg L^{-1} in 2014. SPM was highest at intermediate salinities in the Lumar river, suggesting the existence of an estuarine turbidity maximum (ETM). Particulate organic carbon (POC)

CO₂ and CO emissions from Southeast Asian estuaries

D. Müller et al.

[Title Page](#)

[Abstract](#)

[Introduction](#)

[Conclusions](#)

[References](#)

[Tables](#)

[Figures](#)

[◀](#)

[▶](#)

[◀](#)

[▶](#)

[Back](#)

[Close](#)

[Full Screen / Esc](#)

[Printer-friendly Version](#)

[Interactive Discussion](#)



was higher during the dry season (Table 1), ranging from 51 to $4114 \mu\text{mol L}^{-1}$ in 2013 and from 17 to $2907 \mu\text{mol L}^{-1}$ in 2014. The atomic carbon-to-nitrogen (C/N) ratio of particulate organic matter (POM) ranged between 8.5–14.1 in 2013 and 8.1–13.8 in 2014. $\delta^{13}\text{C}$ values ranged between -28.5 and $-25.5\text{\textperthousand}$ in 2013 and -27.6 to $-24.4\text{\textperthousand}$ in 2014.

In contrast, the C/N ratio in the dissolved organic matter (DOM) was much higher: it ranged between 10.9 and 81.8 (2014 data), whereas the lowest value was measured on the Lumar river, upstream of the Maludam peninsula, and the highest value was measured on the Lumar river at the mouth of a peat-draining left-bank tributary (see Fig. 1). The average for all samples was 40.6.

Since POC was not conservatively transported through the estuary, the export of POC to the South China Sea was estimated from the median POC concentration and discharge (see Supplement). 0.15Tg C yr^{-1} are estimated to be delivered from the Lumar, and another 0.06Tg C yr^{-1} from the Saribas (Table 4). Taken together with the DOC export, this implies that Lumar and Saribas deliver approximately $0.36 \pm 0.30 \text{Tg}$ organic carbon to the South China Sea every year, more than half of which is bound to particles.

3.4 CO_2 and CO

In both years, both CO_2 and CO were found to be above atmospheric equilibrium, indicating that the Lumar and Saribas estuaries were net sources of these gases to the atmosphere.

CO_2 ranged from 297.3 to $5504.0 \mu\text{atm}$ in 2013 and from 326.5 to $5014.1 \mu\text{atm}$ in 2014. CO_2 increased with decreasing salinity, indicating that high CO_2 can be attributed to freshwater input (Fig. 5). However, matters were different for the freshwater samples. The measured freshwater end-member CO_2 was relatively moderate (1021–1527 μatm). Table 2 summarizes the median $p\text{CO}_2$ values in the outer, mid- and upper estuaries. It can be seen that like DOC, CO_2 was highest in the mid-estuaries. The difference between dry and wet season $p\text{CO}_2$ was marginal (see Fig. 5). Although ex-

cess CO_2 (in $\mu\text{mol L}^{-1}$) was weakly correlated with AOU for the individual datasets, higher AOU in the dry season did not concur with higher excess CO_2 (Fig. 6) with the exception of the Saribas tributary (see discussion below).

Interestingly, Saribas and its tributary had a higher CO_2 level (i.e., higher CO_2 at the same salinity) than Lumar, but not higher DOC. $\delta^{13}\text{C-DIC}$ ranged from $-0.85\text{\textperthousand}$ in the lower estuary to $-15.70\text{\textperthousand}$ in the freshwater region and varied approximately linearly with salinity (not shown).

CO ranged from <0.1 to 6.6 nmol L^{-1} in the dry season (2013) and from 0.2 to 12.4 nmol L^{-1} in the wet season (2014) and was spatially variable (Fig. 5). Median values are summarized in Table 2. CO concentrations were higher during daytime than during the night, independent of the boat's location (Fig. 7). In both years, maximum CO concentrations were observed around noon and in the early afternoon. CO concentrations were not correlated with salinity, DOC, POC or SPM (not shown).

3.5 CO_2 and CO fluxes

The CO_2 fluxes measured with the floating chamber showed large spatial variations and ranged from 63 to $935\text{ mmol m}^{-2}\text{ d}^{-1}$. The lowest flux was measured in the Saribas mid-estuary, and the highest flux was measured on the Saribas tributary. k_{600} values were averaged for the individual rivers and are reported with the largest deviation of a single measurement from the mean. The Saribas tributary, which was the smallest of the studied rivers, had the highest k_{600} of $23.9 \pm 14.8\text{ cm h}^{-1}$. The largest river, Lumar, had a high k_{600} of $20.5 \pm 4.9\text{ cm h}^{-1}$ as well, which is probably owed to the high flow velocity (2.5 m s^{-1}). The Saribas main river had a k_{600} of $13.2 \pm 11.0\text{ cm h}^{-1}$, with large spatial variability. The wind speed averaged 3.0 m s^{-1} during our 2013 sampling period and 2.3 m s^{-1} during the 2014 sampling period. The average k_{600} calculated with W92 were one order of magnitude lower than the experimentally determined ones, with 3.1 cm h^{-1} during the dry season and 1.9 cm h^{-1} during the wet season.

Title Page

Abstract

Introduction

Conclusions

References

Tables

Figures

◀

▶

◀

▶

Back

Close

Full Screen / Esc

Printer-friendly Version

Interactive Discussion



Atmospheric $p\text{CO}_2$ averaged 403.6 μatm in the dry season (2013) and 414.4 μatm in the wet season (2014). CO_2 fluxes were calculated for every datapoint using updated solubilities, $p\text{CO}_2$ values and exchange velocities and the average atmospheric partial pressure. The two estimates that were obtained for the two different seasons (2013 spatial extent) were averaged and the uncertainty was estimated from the uncertainty associated with the gas exchange velocity, which proved to cause the largest error. CO fluxes were derived in the same way. Atmospheric CO monthly averages from the NOAA ESRL data set were available from 2004 to 2013. For our dry season data, we used the monthly average for June 2013 (77.91 ppb, corresponding to 77.49 natm), and for our wet season data, we calculated the average CO mixing ratio in March for the years that were available (145.93 ppb, corresponding to 145.58 natm).

The calculated CO_2 and CO fluxes in the outer, mid- and upper estuaries are summarized in Table 3. CO_2 fluxes ranged between 14 and $272 \text{ mol m}^{-2} \text{ yr}^{-1}$ and CO fluxes between 0.8 and $1.9 \text{ mmol m}^{-2} \text{ yr}^{-1}$. Fluxes for the outer estuary were derived for the Lumar river (Fig. 5). Estimates for the upper estuaries were based on our $p\text{CO}_2$ measurements in the freshwater region and the average k_{600} of Lumar and Saribas, respectively (Table 3).

Like $p\text{CO}_2$, the CO_2 fluxes were highest in the mid-estuaries, ranging between 76 and $272 \text{ mol m}^{-2} \text{ yr}^{-1}$. The CO flux from Lumar was twice as high in the mid-estuary than in the outer estuary.

In order to calculate the total flux from these estuaries, we estimated the estuarine surface area of both systems in ArcGIS (for details see Supplement). The Lumar estuary has a surface area of 220 km^2 , which corresponds to 3 % of the catchment area, and the Saribas (excluding the tributary) estuary has a surface area of 102 km^2 (5 % of the catchment). The total flux for the Lumar is 0.31 ± 0.09 and $0.09 \pm 0.08 \text{ Tg Cyr}^{-1}$ for the Saribas (see Table 4). The contribution of CO to these terms is negligible. The contribution of the upper estuaries and rivers was calculated by assuming that they cover 0.89 % of the catchment area (Raymond et al., 2013). For the percentage of the catchment that is covered by peat, we used a previously published estimate for the areal flux

[Title Page](#)[Abstract](#)[Introduction](#)[Conclusions](#)[References](#)[Tables](#)[Figures](#)[◀](#)[▶](#)[◀](#)[▶](#)[Back](#)[Close](#)[Full Screen / Esc](#)[Printer-friendly Version](#)[Interactive Discussion](#)

from a peat-draining river in this region ($F_{\text{peat, areal}} = 167\text{--}386 \text{ mol m}^{-2} \text{ yr}^{-1}$, Müller et al. (2015), we used the average of $277 \pm 110 \text{ mol m}^{-2} \text{ yr}^{-1}$). For the rest, we used the flux that we determined for the upper estuary ($F_{\text{UE, areal}} = 60 \pm 14$ and $33 \pm 28 \text{ mol m}^{-2} \text{ d}^{-1}$ for Lumar and Saribas, respectively). The calculations and the error budget are detailed in the Supplement.

Accordingly, the Lumar upper estuary and river network add $0.09 \pm 0.03 \text{ Tg Cyr}^{-1}$ and the Saribas $0.02 \pm 0.01 \text{ Tg Cyr}^{-1}$ (Table 4). Taken together, the Lumar and Saribas estuaries and rivers release approximately $0.5 \pm 0.2 \text{ Tg CO}_2 \text{--Cyr}^{-1}$ to the atmosphere, approximately 80 % of which comes from the mid-estuaries.

10 4 Discussion

4.1 Sources of carbon in the estuaries

It is striking that both DOC and CO₂ exhibit their maximum concentrations at intermediate salinities, and that the concentration that would be expected for the zero-salinity endmember is overestimated if based on the correlation with salinity. As indicated 15 above, we attribute this to the location of the peatlands. On the northwestern coast of Borneo, tidal intrusion can reach up to 200 km inland (Kselik and Liong, 2004). In the Lumar and Saribas river, saltwater intrusion reaches beyond the extent of the peatlands. Since they likely provide major organic carbon inputs, maximum DOC and CO₂ concentrations are observed at intermediate salinities.

20 The C/N ratios observed in particulate organic matter (POM) were compared to those reported for peat, leaves (Baum, 2008) and phytoplankton (Fig. 4). Accordingly, the C/N in POM (8.1–14.1) is likely a mixed signal from marine and terrestrial sources (Fig. 4), which is in agreement with the relatively low $\delta^{13}\text{C}$ values. The C/N ratios in the dissolved organic matter (DOM) clearly suggest a terrestrial origin (average: 40.6) and 25 are consistent with both plant and peat derived organic matter (Fig. 4). Based on the calculated zero-salinity end-members, we estimated that 15 % of the DOC in the Lumar

[Title Page](#)[Abstract](#)[Introduction](#)[Conclusions](#)[References](#)[Tables](#)[Figures](#)[◀](#)[▶](#)[◀](#)[▶](#)[Back](#)[Close](#)[Full Screen / Esc](#)[Printer-friendly Version](#)[Interactive Discussion](#)

and 3 % of the DOC in the Saribas estuary were derived from peat-draining tributaries. This is not as much as expected, given that peatlands cover 30.5 and 35.5 % of the catchments. Therefore, there must be retention of DOC in the estuary.

4.2 Fate of carbon in the estuaries

5 Likely, a part of the DOC that reaches the Lumar and Saribas estuaries is retained through adsorption and flocculation, which are promoted by mixing of saltwater and freshwater masses. Ertel et al. (1991) found that 1 to 12 % of DOC was converted to POC during laboratory experiments due to changes in salinity. The transformation of DOC to POC in the presence of saltwater was attributed both to particle precipitation
10 and to adsorption of DOM onto riverine particles. Due to the high SPM concentrations in the Lumar and Saribas estuaries, we think that adsorption could be an important process there as well. A partial conversion of DOC to POC is consistent with the high POC concentrations and with the C/N ratios in POM.

15 Additionally, we found evidence that DOC is resired in the estuary. To begin with, like DOC, CO_2 is highest in the mid-estuary. The correlation of AOU and CO_2 and the depletion in $\delta^{13}\text{C}$ -DIC suggest that this CO_2 derives mainly from aerobic respiration of organic matter. This respiration might be promoted by two processes. Firstly, the addition of DOC by peat-draining tributaries contributes substrate for in-situ CO_2 production. Secondly, estuarine CO_2 levels are usually highest in the ETM (Abril and Borges, 2004), where high turbidity limits the light penetration depth and thereby also photosynthetic CO_2 uptake. At the same time, the residence time of organic matter is prolonged (Abril et al., 1999), and particle-attached bacteria get the chance to decompose organic matter (Crump et al., 1998), resulting in pronounced net heterotrophy.

20 25 Although $p\text{CO}_2$ is relatively high, oxygen depletion is quite moderate in comparison. For example, Chen et al. (2008) measured CO_2 partial pressures between 690 to 2680 μatm in the eutrophicated Pearl river estuary (see Table 5) along with AOU up to $239 \mu\text{mol kg}^{-1}$, resulting in hypoxia at the river mouth. Although we found similarly high and even higher $p\text{CO}_2$, oxygen depletion was much less pronounced. This suggests

BGD

12, 8299–8340, 2015

[Title Page](#)

[Abstract](#)

[Introduction](#)

[Conclusions](#)

[References](#)

[Tables](#)

[Figures](#)

◀

▶

◀

▶

[Back](#)

[Close](#)

[Full Screen / Esc](#)

[Printer-friendly Version](#)

[Interactive Discussion](#)



that more oxygen is available in the Luper and Saribas estuaries. Reaeration might be more efficient, i.e. oxygen fluxes across the air–water interface are higher, which could be explained by a high gas exchange velocity, consistent with our measurements, and a shallower water column.

In addition to estuarine respiration, the diurnal CO cycle observed in the Luper and Saribas estuaries (Fig. 7) suggests that photodegradation is another pathway for DOC removal. This diurnal pattern is well known for ocean surface water and explained by a balance of light-dependent production of CO and microbial consumption (Conrad and Seiler, 1980; Conrad et al., 1982; Ohta, 1997). Average CO concentrations in the Luper and Saribas estuaries were lower than in the East China Sea and Yellow Sea (average 2.25 nmol L^{-1} , Yang et al. (2011), see Table 5), which can be attributed to the high turbidity. A high concentration of suspended particulates limits the light penetration depth and increases microbial CO consumption (Law et al., 2002). On the other hand, CO can also be produced by particles (Xie and Zafiriou, 2009), which would have the opposite effect. Since we did not observe a correlation of CO and SPM, this relationship seems to be rather complex. Ultimately, another reason for the low CO concentrations could be that the terrestrial DOM in the Luper and Saribas estuaries is not so susceptible to photodegradation, which would be in contrast to other studies (Valentine and Zepp, 1993; Zhang et al., 2006).

However, it would be too fast to conclude that photochemistry is only of little relevance for the DOM removal in our study area. First of all, most CO is probably produced directly at the water surface and might quickly escape to the atmosphere. We might not have captured this volatile CO fraction with our measurements, since we sampled water from 1 m below the surface. CO concentrations usually decline rapidly with water depth (Ohta et al., 2000), so the numbers presented here can be considered conservative. Secondly, the relevance of photochemistry amounts to more than CO production. Amon and Benner (1996) suggested that photochemical processes play a key role in the breakdown of DOM into compounds that are more readily available for bacterial respiration, such as formaldehyde, acetaldehyde, glyoxylate and pyruvate. However, the

[Title Page](#)[Abstract](#)[Introduction](#)[Conclusions](#)[References](#)[Tables](#)[Figures](#)[◀](#)[▶](#)[◀](#)[▶](#)[Back](#)[Close](#)[Full Screen / Esc](#)[Printer-friendly Version](#)[Interactive Discussion](#)

CO₂ and CO emissions from Southeast Asian estuaries

D. Müller et al.

and the Saribas tributary ($272 \pm 167 \text{ mol m}^{-2} \text{ yr}^{-1}$) are higher than the global average of $37.4 \text{ mol m}^{-2} \text{ yr}^{-1}$ for mid-estuaries (Chen et al., 2012). Similarly, the value reported for small deltas in this region is $41.8 \text{ mol m}^{-2} \text{ yr}^{-1}$ (Laruelle et al., 2013), which is also lower than the fluxes from Lumar and the Saribas tributary. The fluxes from the Saribas mid-estuary appear to be higher than those values, too ($76 \pm 64 \text{ mol m}^{-2} \text{ yr}^{-1}$), but we cannot ascertain this because of the large uncertainty range. Interestingly, the fluxes that we found are also more than one order of magnitude higher than areal fluxes reported for Indian monsoonal estuaries (Sarma et al., 2012) and for other Malaysian rivers (Chen et al., 2013), see Table 5. However, flux estimates depend critically on the gas exchange velocity: both Sarma et al. (2012) and Chen et al. (2013) used the W92 parameterization for calculating the gas exchange velocity. In order to see whether the discrepancy between our results and theirs is a consequence of the different gas exchange velocities used, we recalculated fluxes for our study area using W92 (see Table 5). This way, we obtained fluxes between 2 and $31 \text{ mol m}^{-2} \text{ yr}^{-1}$. The values for the mid-estuaries ($12\text{--}31 \text{ mol m}^{-2} \text{ yr}^{-1}$) are still higher than the values of Chen et al. (2013) and could indicate that the presence of peatlands makes quite a difference for CO₂ emissions from tropical estuaries.

CO flux estimates were in a similar range as those obtained for the Mauritanian upwelling (Kitidis et al., 2011), those reported for the Equatorial Pacific upwelling (Ohta, 1997) and for the East China Sea and Yellow Sea (Yang et al., 2011) (see Table 5). However, if we use our W92 estimates for comparison, it seems that CO fluxes are rather low in our study area, consistent with the observation that CO concentrations appear to be rather low, as discussed above.

Both the CO₂ flux estimates and the CO flux estimates presented in this study and elsewhere depend critically on the gas exchange velocity. The W92 exchange velocities differed considerably from our experimental values, yielding much lower fluxes. We believe that the W92 parameterization, which was derived for the ocean, is not suitable for estuaries, though frequently used. It does not account for the turbulence created by tidal currents and water flow velocity. Borges et al. (2004) showed that the contribution

Title Page	
Abstract	Introduction
Conclusions	References
Tables	Figures
◀	▶
◀	▶
Back	Close
Full Screen / Esc	
Printer-friendly Version	
Interactive Discussion	



of the water-current related gas exchange velocity to the total gas exchange velocity was substantial at low wind speeds, which are prevalent in our case, too. Therefore, we think that it is more accurate to use empirically determined exchange velocities over wind speed parameterizations.

5 The performance of FCs has been a matter of debate. Arguments exist both for FCs leading to over- and underestimation of the flux: because they shield the water surface from wind, they may reduce the gas exchange (Frankignoulle, 1988). However, in our case, the FC-derived exchange velocities were much higher than the W92 ones, so that here, the question is rather whether the FC lead to an overestimation of the flux. This would have been the case if the chamber had created artificial turbulences. Indeed, this has been discussed as one of the major weaknesses of the FC method (Matthews et al., 2003; Vachon et al., 2010), although FCs are more susceptible to disruptions in low-turbulence environments than in high-turbulence environments (Vachon et al., 2010). In contrast, a recent study found a rather good agreement between 10 floating chamber and eddy covariance measurements on a river (Huotari et al., 2013), which suggests that the accuracy of FC measurements is also a matter of design. We intended to avoid creation of artificial turbulence by (1) using short wall extensions of the chamber into the water (ca. 1 cm), which is thought to decrease the artificial turbulence by making the chamber more stable (Matthews et al., 2003), and (2) letting the 15 chamber float freely next to the boat.

Taken together, Lupar and Saribas deliver 0.4 Tg organic carbon to the South China Sea every year and release 0.5 Tg yr^{-1} to the atmosphere as CO_2 . Approximately 20 80 % of the evasion from aquatic systems in the two catchments came from the mid-estuaries. This is noteworthy, since it was recently shown that CO_2 emissions from a blackwater stream on the Maludam peninsula are actually relatively moderate. Müller et al. (2015) showed that due to the short water residence time, 64–84 % of the carbon that this peat-draining river conveyed was exported laterally. Our results imply that a large fraction of this carbon is respiration in the adjacent estuaries and released to the atmosphere.

[Title Page](#)[Abstract](#)[Introduction](#)[Conclusions](#)[References](#)[Tables](#)[Figures](#)[◀](#)[▶](#)[◀](#)[▶](#)[Back](#)[Close](#)[Full Screen / Esc](#)[Printer-friendly Version](#)[Interactive Discussion](#)

Within the uncertainties, we can state that the aquatic CO₂ emissions appear to be approximately as high or higher than the TOC export (Table 4). Since only 15 and 3 % of the DOC in the Lumar and Saribas estuaries were derived from peat-draining tributaries, additional DOC from marine sources or intertidal flats might support net heterotrophy in the estuaries. Another factor adding to the high CO₂ fluxes is the large variability of pH. pH varied spatially by 1.3 (2013) and 0.8 (2014). This can partially be attributed to the inputs from peat-draining rivers, which are highly acidic (Kselik and Liong, 2004; Müller et al., 2015). Lower pH shifts the carbonate system towards more free CO₂, supporting the release of CO₂ to the atmosphere in the mid-estuaries.

Conclusively, while the residence time in the peat-draining tributaries might be insufficient to allow for the transformation of peat-derived organic matter, respiration in the estuary is supported by the prolonged residence time and high oxygen availability. Acidic, high-DOC water from peat-draining tributaries contributes to the emission of large quantities of CO₂ to the atmosphere.

5 Conclusions

Overall, we conclude that these estuaries in a peat-dominated region receive substantial amounts of terrestrial organic carbon, parts of which are contributed by peat-draining tributaries. We found evidence that aerobic respiration removes DOC, resulting in net heterotrophy. Possibly, DOC degradation is supported by photochemistry, but to assess the magnitude and importance of this pathway, further investigation is required. Additionally, we hypothesize that a fraction of the DOC is physically removed by adsorption. This highlights how these estuaries function as an efficient filter between land and ocean. Unlike small peat-draining rivers, which tend to export most organic carbon downstream, the adjacent estuaries seem to trap a large fraction of this terrestrial organic carbon. This means that the carbon export to the continental shelf is reduced, at the price of CO₂ production and, ultimately, emission from the estuary.

[Title Page](#)[Abstract](#)[Introduction](#)[Conclusions](#)[References](#)[Tables](#)[Figures](#)[◀](#)[▶](#)[◀](#)[▶](#)[Back](#)[Close](#)[Full Screen / Esc](#)[Printer-friendly Version](#)[Interactive Discussion](#)

Acknowledgements. We would like to thank the Sarawak Biodiversity Center for permission to conduct research in Sarawak waters (Permit No. SBC-RA-0097-MM and export permit SBC-EP-0040-MM). We thank Hella van Asperen (University of Bremen, Germany), Nastassia Denis, Felicity Kuek, Joanne Yeo, Hong Chang Lim, Edwin Sia (all Swinburne University, Malaysia) and all scientists and students from Swinburne University and the University of Malaysia Sarawak who were involved in the sampling campaigns and the preparation. Lukas Chin and the crew members of the SeaWonder are acknowledged for their extensive support. We would also like to acknowledge Innovasi Samudra Sdn Bhd for the loan of the CTD equipment. The authors thank Matthias Birkicht and Dorothee Dasbach (ZMT Bremen, Germany) for their help in the lab performing the analyses. Ultimately, we acknowledge the University of Bremen for funding this study through the “exploratory project” in the framework of the University’s Institutional Strategy.

15
The article processing charges for this open-access publication
were covered by the University of Bremen.

References

20 Abril, G. and Borges, A. V.: Carbon Dioxide and Methane Emissions from Estuaries, in: Green-
house Gas Emissions: Fluxes and Processes, Hydroelectric Reservoirs and Natural Envi-
ronments, Environmental Science Series, Springer, Berlin, Heidelberg, New York, chapt. 7,
187–207, 2004. 8316

25 Abril, G., Etcheber, H., Hir, P. L., Bassoulet, P., Boutier, B., and Frankignoulle, M.: Oxic/anoxic
oscillations and organic carbon mineralization in an estuarine maximum turbidity zone (the
Gironde, France), Limnol. Oceanogr., 44, 1304–1315, 1999. 8316

Alkhatib, M., Jennerjahn, T. C., and Samiaji, J.: Biogeochemistry of the Dumai River Estu-
ary, Sumatra, Indonesia, a tropical blackwater river, available at: <http://www.jstor.org/stable/4502390> (last access: 3 June 2015), Limnol. Oceanogr., 52, 2410–2417, 2007. 8302

CO₂ and CO emissions from Southeast Asian estuaries

D. Müller et al.

Title Page

Abstract

Introduction

Conclusions

References

Tables

Figures

◀

▶

◀

▶

Back

Close

Full Screen / Esc

Printer-friendly Version

Interactive Discussion



3 Amon, R. M. W. and Benner, R.: Photochemical and microbial consumption of dissolved organic
4 carbon and dissolved oxygen in the Amazon River system, *Geochim. Cosmochim. Ac.*, 60,
5 1783–1792, 1996. 8317

5 Andriesse, J. P.: *Nature and Management of Tropical Peat Soils*, FAO Soils Bulletin 59, Food
6 and Agriculture Organization of the United Nations (FAO), Rome, 1988. 8302

6 Baum, A.: Tropical blackwater biogeochemistry: the Siak River in central Sumatra, Indonesia,
7 PhD thesis, University of Bremen, Bremen, Germany, 2008. 8315, 8337

10 Baum, A., Rixen, T., and Samiaji, J.: Relevance of peat draining rivers in central Sumatra for
8 the riverine input of dissolved organic carbon into the ocean, *Estuar. Coast. Shelf S.*, 73,
11 563–570, 2007. 8302

Borges, A. V., Vanderborght, J.-P., Schiettecatte, L.-S., Gazeau, F., Ferrón-Smith, S., Delille, B.,
12 and Frankignoulle, M.: Variability of the gas transfer velocity of CO₂ in a macrotidal estuary
(the Scheldt), *Estuaries*, 27, 593–603, 2004. 8309, 8319

15 Cai, W.-J.: Estuarine and coastal ocean carbon paradox: CO₂ sinks or sites of terrestrial carbon
16 incineration?, *Annual Reviews of Marine Science*, 3, 123–145, doi:10.1146/annurev-marine-
17 120709-142723, 2011. 8302

Chen, C., Wang, S., Lu, X., Zhang, S., Lui, H., Tseng, H., Wang, B., and Huang, H.: Hydrogeo-
18 chemistry and greenhouse gases of the Pearl River, its estuary and beyond, *Quatern. Int.*,
19 186, 79–90, doi:10.1016/j.quaint.2007.08.024, 2008. 8316, 8333

20 Chen C.-T. A., Huang, T.-H., Fu, Y.-H., Bai, Y., and He, X.: Strong sources of CO₂ in upper
21 estuaries become sinks of CO₂ in large river plumes, *Current Opinion in Environmental Sus-
22 tainability*, 4, 179–185, doi:10.1016/j.cosust.2012.02.003, 2012. 8319

25 Chen, C.-T. A., Huang, T.-H., Chen, Y.-C., Bai, Y., He, X., and Kang, Y.: Air–sea exchanges of
26 CO₂ in the world's coastal seas, *Biogeosciences*, 10, 6509–6544, 2013, doi:10.5194/bg-10-
27 6509-2013. 8307, 8318, 8319, 8333

Conrad, R. and Seiler, W.: Photooxidative production and microbial consumption of carbon
monoxide in seawater, *FEMS Microbiol. Lett.*, 9, 61–64, 1980. 8317

30 Conrad, R. and Seiler, W.: Influence of the surface microlayer on the flux of nonconservative
trace gases (CO, H₂, CH₄, N₂O) across the ocean–atmosphere interface, *J. Atmos. Chem.*,
6, 83–94, 1988.

Conrad, R., Seiler, W., Bunse, G., and Giehl, H.: Carbon monoxide in seawater (Atlantic Ocean),
J. Geophys. Res., 87, 8839–8852, 1982. 8317

**CO₂ and CO
emissions from
Southeast Asian
estuaries**

D. Müller et al.

[Title Page](#)[Abstract](#)[Introduction](#)[Conclusions](#)[References](#)[Tables](#)[Figures](#)[◀](#)[▶](#)[◀](#)[▶](#)[Back](#)[Close](#)[Full Screen / Esc](#)[Printer-friendly Version](#)[Interactive Discussion](#)

Crump, B. C., Baross, J. A., and Simenstad, C. A.: Dominance of particle-attached bacteria in the Columbia River Estuary, USA, *Aquat. Microb. Ecol.*, 14, 7–18, 1998. 8316

Deutscher Wetterdienst (DWD): Climate Data Worldwide, available as Excel-file at: http://www.dwd.de/bvbw/appmanager/bvbw/dwdwwwDesktop?_nfpb=true&_pageLabel=_dwdwww_spezielle_nutzer_energiewirtschaft_historisch&T26607173141161345039102gsbDocumentPath=NavigationFOeffentlichkeitFKlima_UmweltFKlimadatenFKlimadaten_weltweitFdownload_node.htmlF_nnnDtrue (last access: 3 June 2015), 2007. 8303

Dickson, A., Sabine, C., and Christian, J.: Guide to Best Practices for Ocean CO₂ Measurements, PICES Special Publications, 3rd edn., North Pacific Marine Science Organization (PICES), 191 pp., 2007. 8307

Duarte, C. M. and Prairie, Y. T.: Prevalence of heterotrophy and atmospheric CO₂ emissions from aquatic ecosystems, *Ecosystems*, 8, 862–870, doi:10.1007/s10021-005-0177-4, 2005. 8302

Ertel, J. R., Alberts, J. J., and Price, M. T.: Transformation of riverine organic matter in estuaries, in: Proceedings of the 1991 Georgia Water Resources Conference, March 19 and 20, 1991 at the University of Georgia, Athens, Georgia, edited by: Hatcher, K. J., Institute of Natural Resources, The University of Georgia, 309–312, 1991. 8316

FAO: Harmonized World Soil Database, FAO, Rome, Italy and IIASA, Laxenburg, Austria, 2009. 8304, 8334

Frankignoulle, M.: Field measurements of air–sea CO₂ exchange, available at: http://www.aslo.org/lo/toc/vol_33/issue_3/0313.pdf (last access: 3 June 2015), *Limnol. Oceanogr.*, 33, 313–322, 1988. 8320

Grasshoff, K., Kremling, K., and Ehrhardt, M.: Methods of Seawater Analysis, 3rd edn., Verlag Chemie, Wiley-VCH, Weinheim, 1999. 8305

Griffith, D. W. T.: Synthetic calibration and quantitative analysis of gas-phase FT-IR spectra, *Appl. Spectrosc.*, 50, 59–70, 1996. 8306

Griffith, D. W. T., Deutscher, N. M., Caldow, C., Kettlewell, G., Rigganbach, M., and Hammer, S.: A Fourier transform infrared trace gas and isotope analyser for atmospheric applications, *Atmos. Meas. Tech.*, 5, 2481–2498, doi:10.5194/amt-5-2481-2012, 2012. 8306

Hammer, S., Griffith, D. W. T., Konrad, G., Vardag, S., Caldow, C., and Levin, I.: Assessment of a multi-species in situ FTIR for precise atmospheric greenhouse gas observations, *Atmos. Meas. Tech.*, 6, 1153–1170, doi:10.5194/amt-6-1153-2013, 2013. 8306

Title Page	
Abstract	Introduction
Conclusions	References
Tables	Figures
 	 
Back	Close
Full Screen / Esc	
Printer-friendly Version	
Interactive Discussion	



15 Huotari, J., Haapanala, S., Pumpanen, J., Vesala, T., and Ojala, A.: Efficient gas exchange between a boreal river and the atmosphere, *Geophys. Res. Lett.*, 40, 5683–5686, 2013. 8320

20 Jähne, B., Münnich, K. O., Bösinger, R., Dutzi, A., Huber, W., and Libner, P.: On the parameters influencing air–water gas exchange, *J. Geophys. Res.*, 92, 1937–1949, 1987. 8309

25 Johnson, J. E.: Evaluation of a seawater equilibrator for shipboard analysis of dissolved oceanic trace gases, *Anal. Chim. Acta*, 395, 119–132, 1999. 8306, 8307

30 Kitidis, V., Tilstone, G. H., Smyth, T. J., Torres, R., and Law, C. S.: Carbon monoxide emission from a Mauritanian upwelling filament, *Mar. Chem.*, 127, 123–133, doi:10.1016/j.marchem.2011.08.004, 2011. 8319, 8333

35 Kselik, R. A. L. and Liang, T. Y.: Hydrology of the Peat Swamp in Maludam National Park, Bentong Division, Alterra Green World Research, Wageningen, The Netherlands/Forest Department Sarawak, Kuching, Malaysia/Sarawak Forestry Corporation, Kuching, Malaysia, 2004. 8304, 8315, 8321

40 Kumagai, T., Saitoh, T. M., Sato, Y., Takahashi, H., Manfroi, O. J., Morooka, T., Kuraji, K., Suzuki, M., Yasunari, T., and Komatsu, H.: Annual water balance and seasonality of evapotranspiration in a Bornean tropical rainforest, *Agr. Forest Meteorol.*, 128, 81–92, doi:10.1016/j.agrformet.2004.08.006, 2005. 8304, 8310

45 Laruelle, G. G., Dürr, H. H., Lauerwald, R., Hartmann, J., Slomp, C. P., Goossens, N., and Regnier, P. A. G.: Global multi-scale segmentation of continental and coastal waters from the watersheds to the continental margins, *Hydrol. Earth Syst. Sci.*, 17, 2029–2051, doi:10.5194/hess-17-2029-2013, 2013. 8302, 8319

50 Law, C. S., Sjoberg, T. N., and Ling, R. D.: Atmospheric emission and cycling of carbon monoxide in the Scheldt Estuary, available at: <http://www.jstor.org/stable/1469906> (last access: 3 June 2015), *Biogeochemistry*, 59, 69–94, 2002. 8317

55 Lehner, B., Verdin, K., and Jarvis, A.: HydroSHEDS Technical Documentation, available at: <http://hydrosheds.cr.usgs.gov> (last access: 3 June 2015), World Wildlife Funds US, Washington, DC, 1.0 edn., 2006. 8304

60 Liss, P. S. and Merlivat, L.: Air–sea gas exchange rates: introduction and synthesis, in: *The Role of Air–Sea Gas Exchange in Geochemical Cycling*, edited by: Buat-Ménard, P., NATO ASI Series, Reidel, Utrecht, 113–129, 1986. 8333

65 Matthews, C. J. D., St. Louis, V. L., and Hesslein, R. H.: Comparison of three techniques used to measure diffusive gas exchange from sheltered aquatic surfaces, *Environ. Sci. Technol.*, 37, 772–780, doi:10.1021/es0205838, 2003. 8320

Title Page	
Abstract	Introduction
Conclusions	References
Tables	Figures
◀	▶
◀	▶
Back	Close
Full Screen / Esc	
Printer-friendly Version	
Interactive Discussion	



Miller, W. L. and Zepp, R. G.: Photochemical production of dissolved inorganic carbon from terrestrial organic matter: significance to the oceanic organic carbon cycle, *Geophys. Res. Lett.*, 22, 417–420, 1995. 8302

Moore, S., Gauci, V., Evans, C. D., and Page, S. E.: Fluvial organic carbon losses from a borean blackwater river, *Biogeosciences*, 8, 901–909, doi:10.5194/bg-8-901-2011, 2011. 8302, 8318

Moore, S., Evans, C. D., Page, S. E., Garnett, M. H., Jones, T. G., Freeman, C., Hooijer, A., Wiltshire, A. J., Limin, S. H., and Gauci, V.: Deep instability of deforested tropical peatlands revealed by fluvial organic carbon fluxes, *Nature*, 493, 660–664, doi:10.1038/nature11818, 2013. 8302

Müller, D., Warneke, T., Rixen, T., Mueller, M., Jamahari, S., Denis, N., Mujahid, A., and Notholt, J.: Lateral carbon fluxes and CO₂ outgassing from a tropical peat-draining river, *Biogeosciences*, submitted, 2015. 8302, 8311, 8315, 8320, 8321

Nightingale, P. D., Malin, G., Law, C. S., Watson, A. J., Liss, P. S., Liddicoat, M. I., Boutin, J., and Upstill-Goddard, R. C.: In situ evaluation of air–sea gas exchange parameterizations using novel conservative and volatile tracers, *Global Biogeochem. Cy.*, 14, 373–387, 2000. 8333

Noriega, C. and Araujo, M.: Carbon dioxide emissions from estuaries of northern and north-eastern Brazil, *Nature Scientific Reports*, 4, 6164, doi:10.1038/srep06164, 2014. 8333

Novelli, P. C. and Masarie, K. A.: Atmospheric Carbon Monoxide Dry Air Mole Fractions from the NOAA/ESRL Carbon Cycle Cooperative Global Air Sampling Network, 1988–2013, version: 2014-07-02, available at: ftp://aftp.cmdl.noaa.gov/data/trace_gases/co/flask/surface/ (last access: 3 June 2015), NOAA ESRL Global Monitoring Division, Boulder, Colorado, USA, 2014. 8309

Ohta, K.: Diurnal variations of carbon monoxide concentration in the equatorial Pacific upwelling region, *J. Oceanogr.*, 53, 173–178, 1997. 8317, 8319, 8333

Ohta, K., Inomata, Y., Sano, A., and Sugimura, K.: Photochemical degradation of dissolved organic carbon to carbon monoxide in coastal seawater, In: *Dynamics and Characterization of Marine Organic Matter*, edited by: Handa, N., Tanoue, E., and Hama, T., TERRAPUB, Tokyo, 213–229, 2000. 8303, 8317, 8333

Page, S. E., Rieley, J. O., and Banks, C. J.: Global and regional importance of the tropical peatland carbon pool, *Glob. Change Biol.*, 17, 798–818, doi:10.1111/j.1365-2486.2010.02279.x, 2011. 8302

CO₂ and CO emissions from Southeast Asian estuaries

D. Müller et al.

[Title Page](#)

[Abstract](#)

[Introduction](#)

[Conclusions](#)

[References](#)

[Tables](#)

[Figures](#)

◀

▶

◀

▶

[Back](#)

[Close](#)

[Full Screen / Esc](#)

[Printer-friendly Version](#)

[Interactive Discussion](#)



CO₂ and CO emissions from Southeast Asian estuaries

D. Müller et al.

[Title Page](#)

[Abstract](#)

[Introduction](#)

[Conclusions](#)

[References](#)

[Tables](#)

[Figures](#)

◀

▶

◀

▶

[Back](#)

[Close](#)

[Full Screen / Esc](#)

[Printer-friendly Version](#)

[Interactive Discussion](#)



Weiss, R. F. and Price, B. A.: Nitrous oxide solubility in water and seawater, *Mar. Chem.*, 8, 347–359, 1980. 8307

Wiesenburg, D. A. and Guinasso Jr., N. L.: Equilibrium solubilities of methane, carbon monoxide, and hydrogen in water and seawater, *J. Chem. Eng. Data*, 24, 356–360, 1979. 8308

5 Xie, H. and Zafiriou, O. C.: Evidence for significant photochemical production of carbon monoxide by particles in coastal and oligotrophic marine waters, *Geophys. Res. Lett.*, 36, L23606, doi:10.1029/2009GL041158, 2009. 8317

10 Yang, G.-P., Ren, C.-Y., Lu, X.-L., Liu, C.-Y., and Ding, H.-B.: Distribution, flux, and photoproduction of carbon monoxide in the East China Sea and Yellow Sea in spring, *J. Geophys. Res.*, 116, C02001, doi:10.1029/2010JC006300, 2011. 8317, 8319, 8333

Zafiriou, O. C., Xie, H., Nelson, N. B., Najjar, R. G., and Wang, W.: Diel carbon monoxide cycling in the upper Sargasso Sea near Bermuda at the onset of spring and in midsummer, *Limnol. Oceanogr.*, 53, 835–850, 2008. 8309

15 Zhai, W., Dai, M., Cai, W.-J., Wang, Y., and Wang, Z.: High partial pressure of CO₂ and its maintaining mechanism in a subtropical estuary: the Pearl River Estuary, China, *Mar. Chem.*, 93, 21–32, doi:10.1016/j.marchem.2004.07.003, 2005.

Zhang, Y., Xie, H., and Chen, G.: Factors affecting the efficiency of carbon monoxide photoproduction in the St. Lawrence estuarine system (Canada), *Environ. Sci. Technol.*, 40, 7771–7777, doi:10.1021/es0615268, 2006. 8303, 8317

CO₂ and CO emissions from Southeast Asian estuaries

D. Müller et al.

[Title Page](#)

[Abstract](#)

[Introduction](#)

[Conclusions](#)

[References](#)

[Tables](#)

[Figures](#)

◀

▶

◀

▶

[Back](#)

[Close](#)

[Full Screen / Esc](#)

[Printer-friendly Version](#)

[Interactive Discussion](#)



Table 1. Dissolved organic carbon (DOC), particulate organic carbon (POC) and dissolved inorganic nitrogen (DIN) median concentrations and oxygen saturation in the Lumar and Saribas estuary.

	DOC ($\mu\text{mol L}^{-1}$)		POC ($\mu\text{mol L}^{-1}$)		DIN ($\mu\text{mol L}^{-1}$)		DO (%)	
	dry	wet	dry	wet	dry	wet	dry	wet
Lumar OE	142*	n.d.	62*	n.d.	7*	n.d.	n.d.	n.d.
Saribas OE	n.d.	244*	n.d.	42*	n.d.	18*	n.d.	100.4*
Lumar ME	340	338	456	650	22	20	70.8	94.4
Saribas ME	258	281	766	292	30	14	82.8	85.8
Saribas tributary	685	374	2040	281	22	11	n.d.	82.8
Lumar UE	89	208	79	131	5	5	84.4	93.3
Saribas UE	312*	n.d.	4114*	n.d.	19*	n.d.	63.6*	n.d.

OE: Outer estuaries (salinity > 25).

ME: Mid-estuaries (salinity 2–25, for the 2013 spatial extent of the rivers).

UE: upper estuaries.

* denotes that only one data point was available.

[Title Page](#)

[Abstract](#)

[Introduction](#)

[Conclusions](#)

[References](#)

[Tables](#)

[Figures](#)

◀

▶

◀

▶

[Back](#)

[Close](#)

[Full Screen / Esc](#)

[Printer-friendly Version](#)

[Interactive Discussion](#)



Table 2. Median CO₂ partial pressures and CO concentrations, respectively.

	pCO ₂ (μatm)		CO (nmol L ⁻¹)	
	dry	wet	dry	wet
Lupar OE	618 ± 44	662 ± 36	0.3 ± 0.1	0.7 ± 0.1
Saribas OE	n.d.	n.d.	n.d.	n.d.
Lupar ME	2461 ± 574	1849 ± 881	1.4 ± 1.1	0.5 ± 2.7
Saribas ME	2240 ± 442	2235 ± 304	0.5 ± 0.9	0.7 ± 0.7
Saribas tributary	5064 ± 840	2925 ± 789	0.5 ± 0.7	0.4 ± 0.5
Lupar UE	1527 ± 38	1021 ± 357	n.d.	n.d.
Saribas UE	1159 ± 29	n.d.	n.d.	n.d.

OE: Outer estuaries (salinity > 25).

ME: Mid-estuaries (salinity 2–25, for the 2013 spatial extent of the rivers).

UE: upper estuaries.

Values are median ± one standard deviation.

- [Title Page](#)
- [Abstract](#) [Introduction](#)
- [Conclusions](#) [References](#)
- [Tables](#) [Figures](#)
- [◀](#) [▶](#)
- [◀](#) [▶](#)
- [Back](#) [Close](#)
- [Full Screen / Esc](#)
- [Printer-friendly Version](#)
- [Interactive Discussion](#)



Table 3. CO₂ and CO fluxes measured in the Lumar and Saribas estuaries.

	<i>F</i> CO ₂ (mol m ⁻² yr ⁻¹)			<i>F</i> CO (mmol m ⁻² yr ⁻¹)	
	OE	ME	UE	OE	ME
Lumar	14 ± 3	119 ± 28	60 ± 14	0.9 ± 0.2	1.9 ± 0.5
Saribas	n.d.	76 ± 64	33 ± 28	n.d.	0.8 ± 0.6
Saribas tributary	n.d.	272 ± 167	n.d.	n.d.	0.9 ± 0.6

OE: Outer estuaries (salinity > 25).

ME: Mid-estuaries (salinity 2–25, for the 2013 spatial extent of the rivers).

UE: upper estuaries.

Table 4. Total CO₂ fluxes estimated for the Lumar and Saribas aquatic systems. All numbers are in TgCyr⁻¹.

	Lumar	Saribas	Total
CO ₂ emissions from rivers (peat)	0.06 ± 0.02	0.02 ± 0.01	0.08 ± 0.03
CO ₂ emissions from UE and rivers (non-peat)	0.03 ± 0.01	< 0.01	0.03 ± 0.01
Total riverine CO ₂ emissions	0.09 ± 0.03	0.02 ± 0.01	0.11 ± 0.04
Estuarine CO ₂ emissions	0.31 ± 0.09	0.09 ± 0.08	0.40 ± 0.17
Total aquatic emissions	0.40 ± 0.12	0.12 ± 0.10	0.52 ± 0.22
DOC export	0.12 ± 0.05	0.03 ± 0.01	0.15 ± 0.05
POC export	0.15 ± 0.18	0.06 ± 0.07	0.21 ± 0.25
TOC export	0.27 ± 0.23	0.09 ± 0.07	0.36 ± 0.30



Title Page

Abstract

Introduction

Conclusions

References

Tables

Figures

◀

▶

◀

▶

Back

Close

Full Screen / Esc

Printer-friendly Version

Interactive Discussion

Title Page

Abstract

Introduction

Conclusions

References

Tables

Figures

◀

▶

◀

▶

Back

Close

Full Screen / Esc

Printer-friendly Version

Interactive Discussion



Table 5. Comparison of CO₂ and CO values for partial pressure and concentration, respectively, and fluxes for different tropical and subtropical sites.

CO ₂ Site	<i>p</i> CO ₂ (μatm)	<i>FC</i> CO ₂ (mol m ⁻² yr ⁻¹)	<i>k</i> model	Reference
outer estuaries in Sarawak, MY	618–662	14 2	FC W92	This study
mid-estuaries in Sarawak, MY	1849–5064	76–272 12–31	FC W92	This study
upper estuaries in Sarawak, MY	1021–1527	33–60 6–7	FC W92	This study
Malaysian estuaries	n.d.	0.4–6.3	W92	Chen et al. (2013)
Indonesian estuaries	n.d.	8.5–54.1	W92	Chen et al. (2013)
Pearl river estuary, CN	690–2680	n.d.	n.d.	Chen et al. (2008)
Brazilian estuaries	162–8638	0.3–63.9	RC01	Noriega and Araujo (2014)
Indian estuaries	300–18 492	–0.01–132.1	W92	Sarma et al. (2012)
CO Site	CO (nmol L ⁻¹)	<i>FC</i> CO (mmol m ⁻² yr ⁻¹)	<i>k</i> model	Reference
outer estuaries in Sarawak, MY	0.3–0.7 < 0.1	0.9 0.8–1.9	FC W92	This study
mid-estuaries in Sarawak, MY	0.4–1.4 0.1–0.3	0.8–1.9 0.7–4.0	FC W92	This study
Seto Inland Sea and Ise Bay, JP	n.d.	0.7–4.0	LM86	Ohta et al. (2000)
Equatorial Pacific	1.9–7.7	1.4–1.6	LM86	Ohta (1997)
Mauritanian upwelling	0.1–6.2	1.7–3.5	N00	Kitidis et al. (2011)
East China and Yellow Sea	0.1–7.0	0.4–6.8	W92	Yang et al. (2011)

The gas exchange velocity *k* used to calculate the flux was determined using different approaches:

FC = floating chamber measurements.

W92 = Wanninkhof (1992).

N00 = Nightingale et al. (2000).

LM86 = Liss and Merlivat (1986).

RC01 = Raymond and Cole (2001).

CO₂ and CO emissions from Southeast Asian estuaries

D. Müller et al.

Title Page

Abstract

Introduction

Conclusions

References

Tables

Figures

Map showing the locations of sampling stations (black dots) along the Saribas, Maludam, and Lupar rivers. The rivers are shaded green, indicating the presence of peat. The inset map shows the location of the study area in Sarawak, Malaysia.

Legend:

- Stations covered in both years
- Stations June 2013
- Stations March 2014
- PEAT

Figure 1. Map of the study area. The stations are indicated by the grey and black dots, peat soils (histosols) are indicated in green (as of FAO, 2009).

CO₂ and CO emissions from Southeast Asian estuaries

D. Müller et al.

Title Page

Abstract

Introduction

Conclus

References

Table

Figures

14

4

1

1

Back

Class

Full Screen / Esc

[Printer-friendly Version](#)

Interactive Discussion

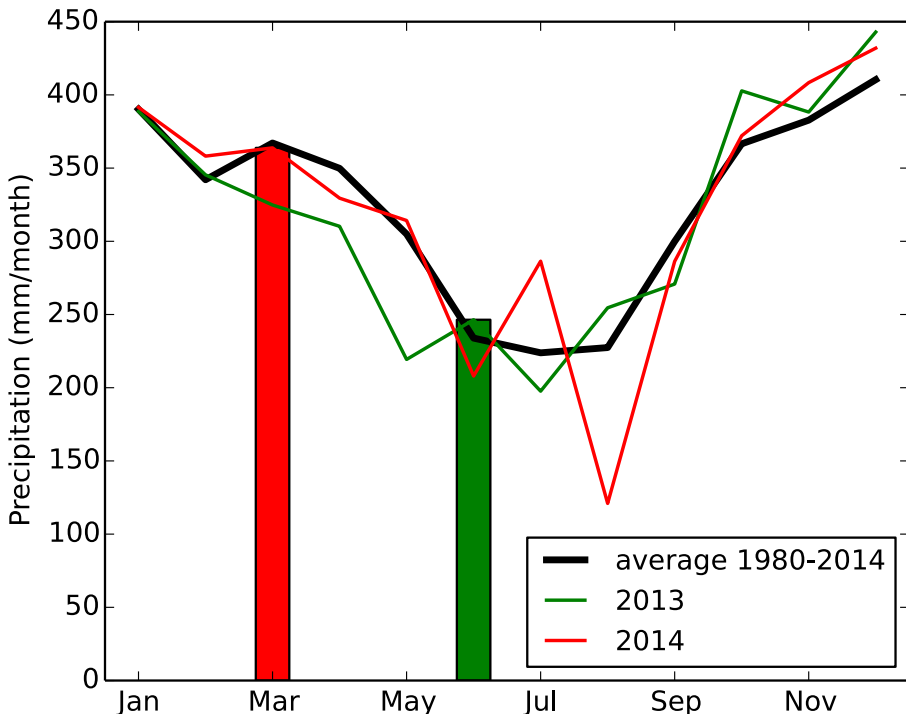


Figure 2. Average monthly precipitation during 1980–2014 (black), monthly precipitation in 2013 (green) and 2014 (red). The bars indicate the rainfall during our sampling months. It can be seen that the rainfall pattern was not much different from the historical average during these periods.

CO₂ and CO emissions from Southeast Asian estuaries

D. Müller et al.

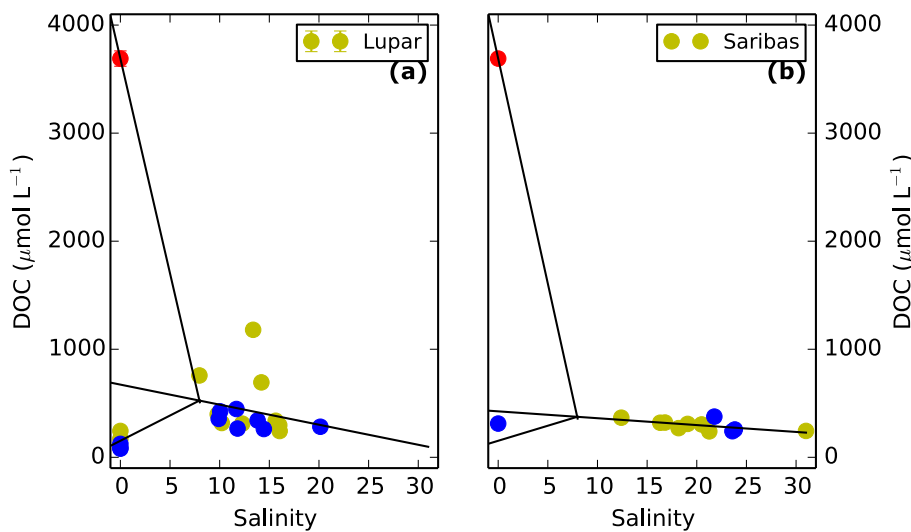


Figure 3. Dissolved organic carbon (DOC) concentrations vs. salinity in the Lumar **(a)** and Saribas **(b)** estuaries. The red marker refers to the zero salinity end-member in the peat-draining tributaries. The lines indicate mixing of the different water masses.

CO₂ and CO emissions from Southeast Asian estuaries

D. Müller et al.

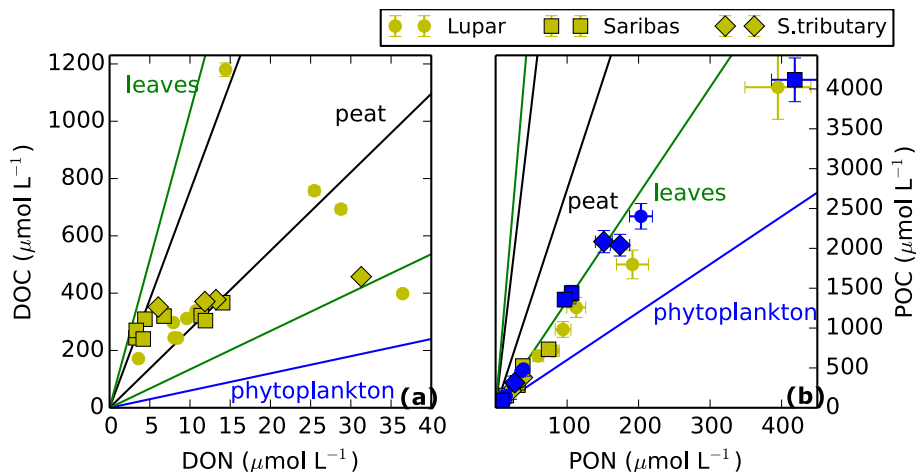


Figure 4. Carbon-to-nitrogen (C/N) ratios in dissolved organic matter **(a)** and in particulate organic matter **(b)**. Blue markers refer to samples from 2013, yellow markers refer to samples from 2014. The individual rivers are denoted by different symbols. Lines refer to the C/N ratios that would be expected for tropical peat and leaves (Baum, 2008) and for phytoplankton.

CO₂ and CO emissions from Southeast Asian estuaries

D. Müller et al.

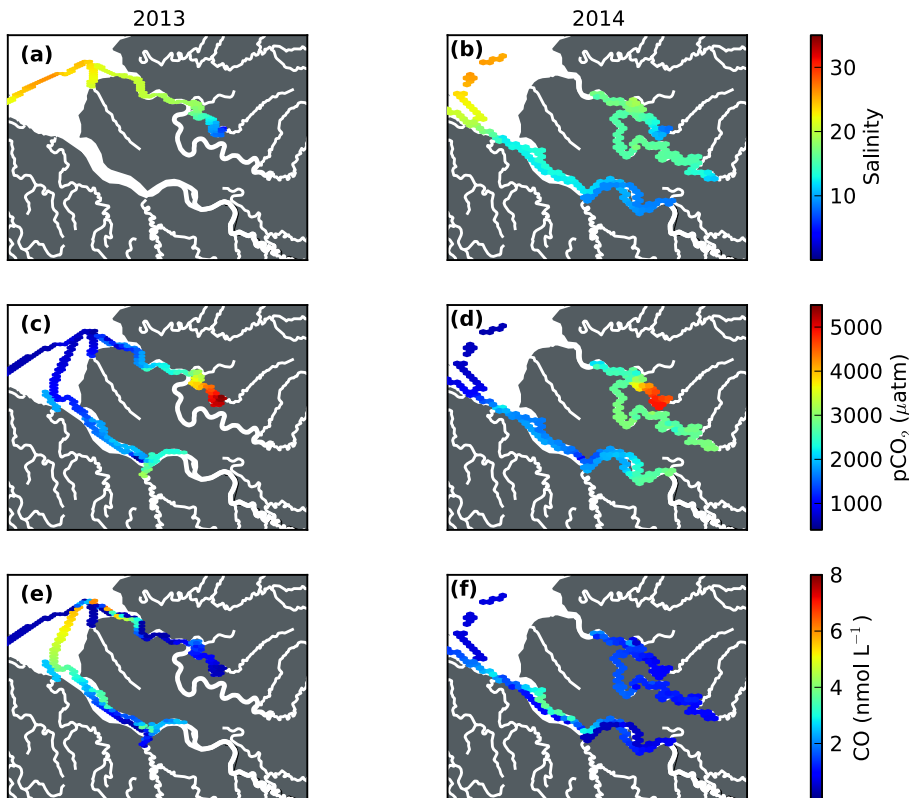


Figure 5. Salinity (a and b), CO₂ partial pressures (c and d) and CO concentrations (e and f) measured during the two cruises in 2013 (left column) and 2014 (right column).

Figure 6. Apparent oxygen utilization (AOU) vs. excess CO₂. Blue markers refer to samples from 2013, yellow markers refer to samples from 2014. The individual rivers are denoted by different symbols.

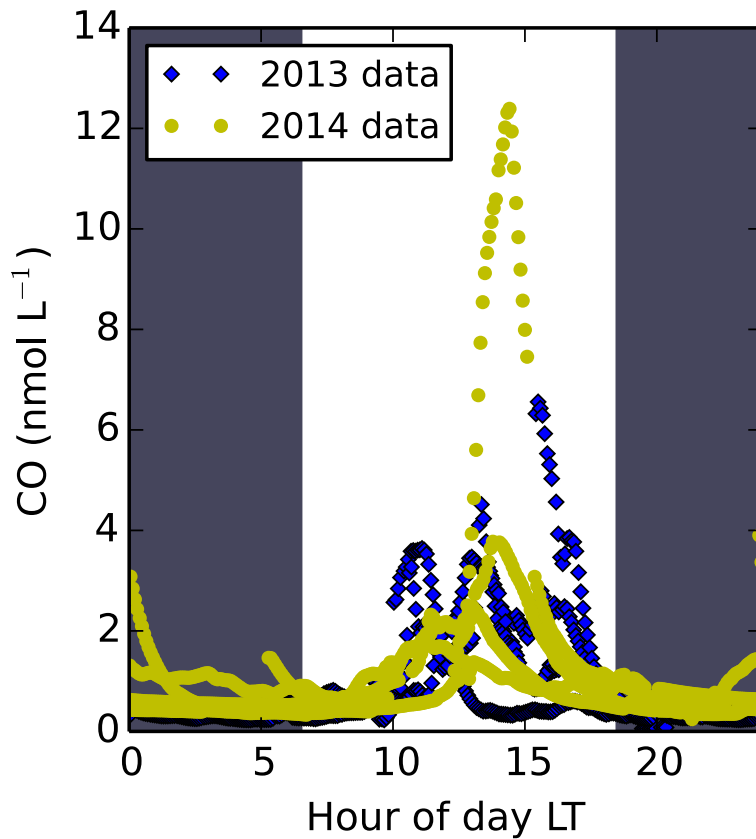


Figure 7. CO concentrations depending on the hour of the day local time. The black areas refer to night-time hours, while the light area denotes the daylight hours. All data are gathered in this figure, 2013 and 2014 data are distinguished with different colors and symbols.